
This copy is for your personal, non-commercial use only.

If you wish to distribute this article to others, you can order high-quality copies for your colleagues, clients, or customers by [clicking here](#).

Permission to republish or repurpose articles or portions of articles can be obtained by following the guidelines [here](#).

The following resources related to this article are available online at www.sciencemag.org (this information is current as of September 25, 2014):

Updated information and services, including high-resolution figures, can be found in the online version of this article at:

<http://www.sciencemag.org/content/345/6204/1609.full.html>

Supporting Online Material can be found at:

<http://www.sciencemag.org/content/suppl/2014/09/24/345.6204.1609.DC1.html>

<http://www.sciencemag.org/content/suppl/2014/09/24/345.6204.1609.DC2.html>

A list of selected additional articles on the Science Web sites **related to this article** can be found at:

<http://www.sciencemag.org/content/345/6204/1609.full.html#related>

This article **cites 133 articles**, 6 of which can be accessed free:

<http://www.sciencemag.org/content/345/6204/1609.full.html#ref-list-1>

This article appears in the following **subject collections**:

Anthropology

<http://www.sciencemag.org/cgi/collection/anthro>

directly or indirectly through the BZR1 family) leads to higher BIN2 activity and derepression of SPCH, promoting accumulation of SPCH in active meristemoids (Fig. 4F). Overall, this feedback mechanism by SPCH would serve to reinforce differences between SPCH-expressing meristemoids and nonexpressing neighbors, which may be important for local patterning and coordinating the lineage with overall BR-mediated growth controls.

Here, we revealed the broad influence of SPCH in stomatal lineage specification through MOBE-ChIP. This technique, which is based on a simple scale increase, could be widely applicable in other tissues or organisms to obtain high-quality binding information about cell-type-specific regulators. The large number of SPCH-binding regions reported here is reminiscent of the behavior of the bHLH transcription factor MyoD, a master regulator of mammalian myogenesis, which associates with more than 30,000 regions in the human genome and is responsible for resetting global transcriptional and epigenetic states during development (29). Additional experiments are needed to establish definitively how often and by what mechanisms SPCH binding alters gene expression. However, our data that hundreds of genes, including those mediating abiotic and hormone responses, are directly regulated by SPCH supports previous functional studies (20, 22) that place SPCH in a critical position to integrate physiological and environmental information into a developmental program that optimizes leaf properties (stomatal density and size) for prevailing environments.

REFERENCES AND NOTES

- R. Heidstra, S. Sabatini, *Nat. Rev. Mol. Cell Biol.* **15**, 301–312 (2014).
- A. P. Fong, S. J. Tapscott, *Curr. Opin. Genet. Dev.* **23**, 568–573 (2013).
- A. Garcia-Bellido, J. F. de Celis, *Genetics* **182**, 631–639 (2009).
- O. S. Lau, D. C. Bergmann, *Development* **139**, 3683–3692 (2012).
- L. J. Pillitteri, J. Dong, *Arabidopsis Book* **11**, e0162 (2013).
- S. Robinson *et al.*, *Science* **333**, 1436–1440 (2011).
- C. A. MacAlister, K. Ohashi-Ito, D. C. Bergmann, *Nature* **445**, 537–540 (2007).
- L. J. Pillitteri, D. B. Sloan, N. L. Bogenschutz, K. U. Torii, *Nature* **445**, 501–505 (2007).
- J. M. Muiño, K. Kaufmann, R. C. van Ham, G. C. Angenent, P. Krajewski, *Plant Methods* **7**, 11 (2011).
- K. Schiessl, J. M. Muiño, R. Sablowski, *Proc. Natl. Acad. Sci. U.S.A.* **111**, 2830–2835 (2014).
- K. Kaufmann *et al.*, *Science* **328**, 85–89 (2010).
- J. Dong, C. A. MacAlister, D. C. Bergmann, *Cell* **137**, 1320–1330 (2009).
- L. J. Pillitteri, K. M. Peterson, R. J. Horst, K. U. Torii, *Plant Cell* **23**, 3260–3275 (2011).
- M. M. Kanaoka *et al.*, *Plant Cell* **20**, 1775–1785 (2008).
- J. A. Nadeau, F. D. Sack, *Science* **296**, 1697–1700 (2002).
- E. D. Shpak, J. M. McAbee, L. J. Pillitteri, K. U. Torii, *Science* **309**, 290–293 (2005).
- L. Hunt, J. E. Gray, *Curr. Biol.* **19**, 864–869 (2009).
- J. L. Malcos, R. J. Cyr, *Cytoskeleton (Hoboken)* **68**, 247–258 (2011).
- C. G. Rasmussen, J. A. Humphries, L. G. Smith, *Annu. Rev. Plant Biol.* **62**, 387–409 (2011).
- J. Le *et al.*, *Nat. Commun.* **5**, 3090 (2014).
- T.-W. Kim, M. Michniewicz, D. C. Bergmann, Z.-Y. Wang, *Nature* **482**, 419–422 (2012).
- G. E. Gudesblat *et al.*, *Nat. Cell Biol.* **14**, 548–554 (2012).
- Y. Tanaka, T. Nose, Y. Jikumaru, Y. Kamiya, *Plant J.* **74**, 448–457 (2013).
- M. Szekestes *et al.*, *Cell* **85**, 171–182 (1996).
- Z. Y. Wang *et al.*, *Dev. Cell* **2**, 505–513 (2002).
- Y. Yin *et al.*, *Cell* **109**, 181–191 (2002).
- Y. Yin *et al.*, *Cell* **120**, 249–259 (2005).
- J.-X. He *et al.*, *Science* **307**, 1634–1638 (2005).
- Y. Cao *et al.*, *Dev. Cell* **18**, 662–674 (2010).

ACKNOWLEDGMENTS

We thank Z.-Y. Wang (Carnegie) for the antibody to YFP and the *bin2-1* allele; Y. Yin (Iowa State University) for the BES1pro: *bes1-D-GFP* construct; J. Chory (SALK) for the *bes1* RNAi line; and members of our laboratory for critical comments. Funding for this work was provided by National Institutes of Health (NIH) 1R01GM086632. O.S.L. was a Croucher Fellow, K.A.D. was supported by Cellular and Molecular Biology Training Program NIH5T32GM007276 and by a National Science Foundation

graduate research fellowship, and J.A. was supported by the DAAD. D.C.B. is a Gordon and Betty Moore Foundation Investigator of the Howard Hughes Medical Institute. The ChIP-seq and RNA-seq data in this study can be found in National Center for Biotechnology Information's Gene Expression Omnibus repository (www.ncbi.nlm.nih.gov/geo) as GSE57954. The supplementary materials contain additional data.

SUPPLEMENTARY MATERIALS

www.sciencemag.org/content/345/6204/1605/suppl/DC1
Materials and Methods
Figs. S1 to S15
Tables S1 to S8
References (30–62)

3 June 2014; accepted 25 August 2014
Published online 4 September 2014;
10.1126/science.1256888

PALEOLITHIC TOOLS

Early Levallois technology and the Lower to Middle Paleolithic transition in the Southern Caucasus

D. S. Adler,^{1*} K. N. Wilkinson,² S. Blockley,³ D. F. Mark,⁴ R. Pinhasi,⁵ B. A. Schmidt-Magee,¹ S. Nahapetyan,⁶ C. Mallol,⁷ F. Berna,⁸ P. J. Glauberman,¹ Y. Raczynski-Henk,⁹ N. Wales,^{1,10} E. Frahm,¹¹ O. Jöris,¹² A. MacLeod,³ V. C. Smith,¹³ V. L. Cullen,¹³ B. Gasparian¹⁴

The Lower to Middle Paleolithic transition (~400,000 to 200,000 years ago) is marked by technical, behavioral, and anatomical changes among hominin populations throughout Africa and Eurasia. The replacement of bifacial stone tools, such as handaxes, by tools made on flakes detached from Levallois cores documents the most important conceptual shift in stone tool production strategies since the advent of bifacial technology more than one million years earlier and has been argued to result from the expansion of archaic *Homo sapiens* out of Africa. Our data from Nor Geghi 1, Armenia, record the earliest synchronic use of bifacial and Levallois technology outside Africa and are consistent with the hypothesis that this transition occurred independently within geographically dispersed, technologically precocious hominin populations with a shared technological ancestry.

The Late Middle Pleistocene [LMP, oxygen isotope stage (OIS) 12/11e to OIS 6/5e, ~425 to 130 thousand years ago (ka)] witnessed the evolution of *Homo sapiens* in Africa and Neandertals in western Eurasia (1, 2). In Africa, the Early Stone Age (ESA)–Middle Stone Age (MSA) transition is characterized by the slow replacement of bifaces by flakes, points, and blades produced through various hierarchical core reduction strategies, among which Levallois concepts are the most notable (3–6). In Western Europe, lithic assemblages from Late Acheulean contexts highlight the asynchronous, geographically discontinuous evolution from bifacial to Levallois technology and the gradual transition from the Lower Paleolithic (LP) to the Middle Paleolithic (MP) ~300 to 200 ka (7–9). Levantine sites assigned to the Acheulo-Yabrudian (AY, ~400 to 200 ka) document non-Levallois methods for the manufacture of blades, broad flakes, and thick scrapers with scalar retouch (Quina) and the gradual disappearance of bifaces (10, 11). The techno-

logical variability apparent in these regions reflects the complex hominin behavioral mosaic in place before the MSA and the MP (12) (Fig. 1). Within the Southern Caucasus, a region situated between Africa and Europe, this critical period of technological and behavioral evolution remains uncharted and undated (13).

In bifacial technology (Mode 2), a mass of stone is shaped through the serial removal of inter-related flakes (façonnage) until the remaining volume takes on a desired form, such as a handaxe. This method of stone tool production originated in Africa ~1.75 million years ago and spread to Eurasia with the initial Acheulean dispersal <900 ka. In contrast, Levallois technology (Mode 3), a specific hierarchical core reduction strategy, entails the multistage shaping (façonnage) of a mass of stone (core) in preparation to detach a flake of predetermined size and shape from a single preferred surface (débitage) (14, 15). Flakes resulting from biface production were generally treated as waste, whereas particular flakes detached from a

Levallois core are the desired products. The novel combination of the shaping and flaking systems in Levallois technology during the Late Acheulian and the eventual replacement of bifacial technology by Levallois methods denote the beginning of the MSA/MP.

In Levallois technology, the volume of the core is conceived as two hierarchically related surfaces separated by a plane of intersection, with the upper, or flake release surface representing the exploitable volume and the lower, or striking platform surface representing the unexploited volume (14, 15). The flake release surface is shaped through the management of lateral and distal convexities so as to control the morphology of the resulting products (flakes), and the flake release surface is parallel to the plane of intersection. The intersection between the flake release surface and the striking platform is perpendicular to the axis of percussion, and all stages of reduction are achieved through hard-hammer percussion.

Levallois technology is subdivided into the preferential method, in which a single Levallois flake is produced before the reparation of core convexities, and the recurrent method, in which multiple Levallois flakes are detached before reparation (14, 15). Core convexities are created through the detachment of preparatory flakes (e.g., débordants), which in turn influence the pattern of detachments from the flake release surface. Three main patterns are typically observed among Levallois cores and flakes: removals from one direction (unidirectional, parallel, or convergent), from two directions (opposed or orthogonal), or along the circumference of the core (radial or centripetal).

Recent studies highlight a specific set of multiple functional/adaptive advantages, or “coinciding optima” (16–18), that might help explain the broad temporal and geographic distribution

of Levallois reduction methods after OIS 8. For example, Levallois technology is shown to be optimal in terms of raw material economy and flake utility (17), and Levallois flakes detached from preferential Levallois cores form a statistically robust group with morphologically desirable characteristics that are distinguishable from those of other flakes (19).

The diffusion of ideas or movement of populations is routinely implicated in the distribution of Levallois technology, with some scholars arguing that its geographic proliferation in Eurasia was predicated on the expansion of archaic *Homo sapiens* from Africa (20). This and allied hypotheses imply that the appearance of Levallois technology outside Africa was sudden, reflecting a

behavioral, if not an actual biological replacement event. Therefore, technological discontinuity with the preceding Acheulian (Mode 2) is to be expected. Such hypotheses also assume direct correlations between specific hominin species and certain stone tool technologies, with movements of the former taken to explain complex geographic and temporal patterns in material culture evolution and distribution (20–22). These expectations and assumptions are ill suited to the LMP, during which the poorly sampled archaeological record exhibits substantial technological variability across great spans of time and space, the sparse chronometric record is of limited accuracy and precision, and significant variability in the ancient DNA and hominin fossil records

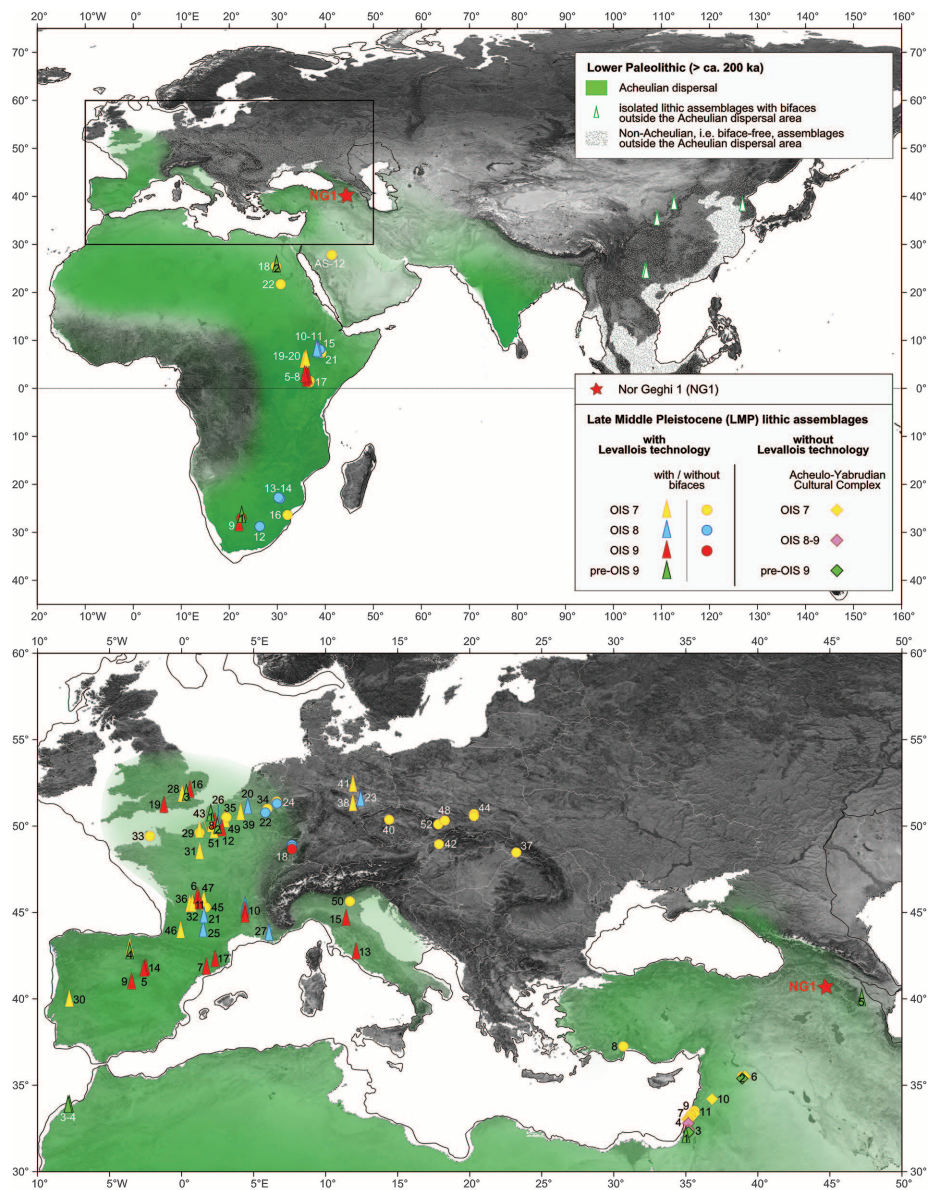


Fig. 1. Spatiotemporal distribution of early Levallois and biface technology during the LMP (>200 ka, >OIS 9 to OIS 7) in the Old World. Data are correlated with table S6, which provides detailed information on each site. The inset illustrates the spatiotemporal distribution of the Eurasian data correlated with technology. Landmasses conform to modern coastlines, and ancient coastlines are drawn to ~ -75 m (average glacial levels). Ice cover is not depicted. The background map is modified after (37).

¹Department of Anthropology, University of Connecticut, 354 Mansfield Road, Unit 1176, Storrs, CT 06269, USA.

²Department of Archaeology, University of Winchester, Winchester, SO22 4NR, UK. ³Department of Geography, Royal Holloway, University of London, Egham, Surrey, TW20 0EX, UK. ⁴Natural Environment Research Council Argon Isotope Facility, Scottish Universities Environmental Research Centre, Scottish Enterprise and Technology Park, Rankine Avenue, East Kilbride, G75 0QF, UK. ⁵School of Archaeology, University College Dublin, Newman Building, Belfield, Dublin 4, Ireland. ⁶Department of Cartography and Geomorphology, Yerevan State University, Alek Manukyan 1, 0025 Yerevan, Armenia. ⁷Departamento de Geografía e Historia, Universidad de La Laguna, Tenerife, Spain. ⁸Department of Archaeology, Simon Fraser University, 8888 University Drive, Burnaby, British Columbia, V5A 1S6, Canada. ⁹Ex-Situ Silex, Leiden, Netherlands. ¹⁰Centre for GeoGenetics, University of Copenhagen, Øster Voldgade 5-7, 1350 Copenhagen K, Denmark. ¹¹Department of Archaeology, University of Sheffield, Northgate House, West Street, Sheffield, S1 4ET, UK. ¹²MONREPOS Archaeological Research Centre and Museum for Human Behavioural Evolution, Römisch-Germanisches Zentralmuseum Mainz, Schloss Monrepos, D-56567 Neuwied, Germany. ¹³Research Laboratory for Archaeology and the History of Art, University of Oxford, Dyson Perrins Building, South Parks Road, Oxford, OX1 3QY, UK. ¹⁴Institute of Archaeology and Ethnology, National Academy of Sciences of the Republic of Armenia, Charents 15, 0025 Yerevan, Armenia.

*Corresponding author. E-mail: daniel.adler@uconn.edu

defy simple taxonomic attributions (23, 24). Our research at Nor Geghi 1 (NG1), a stratified Late Acheulian open-air site at the edge of the Armenian Volcanic Highlands (Fig. 1 and fig. S1), challenges the single-origin and dispersal hypothesis by providing the earliest evidence outside Africa for a transitional site at which hominins engaged in the simultaneous practice of bifacial and Levallois technology (25).

NG1 was discovered in 2008 when obsidian artifacts were found eroding from a 135-m-long section exposed on the western wall of the Hrazdan Gorge (40°20.8'N, 44°35.823'E, 1375 m above sea level). The Hrazdan River connects Lake Sevan (36 km north) with the Arax River (38 km southwest), and in its central 40-km stretch the Hrazdan cuts through basaltic lava flows emanating from volcanoes in the western part of the Gegham range (fig. S1). A broad chronology for these flows is provided by $^{40}\text{K}/^{40}\text{Ar}$ and $^{40}\text{Ar}/^{39}\text{Ar}$ dating of lavas from the Hatis, Gutanasar, and Mensakar volcanoes, suggesting that the vents formed ~700 ka and had eruptive histories spanning ~550,000 to 200,000 years (26–28).

The archaeology of NG1 is contained within alluvial sediments sandwiched between an upper (Basalt 1) and a lower (Basalt 7) lava flow (figs. S2 to S5). The $^{40}\text{Ar}/^{39}\text{Ar}$ technique was used to date Basalt 7 (441 ± 6 ka) and Basalt 1 (197 ± 7 ka) (fig. S8 and database S2), thereby bracketing the stratified alluvial sediments between late OIS 12 and the end of OIS 7 (Fig. 2). The five stratigraphic units recorded between the basalts (from bottom to top, Units 5 to 1) form a normally bedded sequence of fine-grained sedimentary beds, with a minor proportion of sands and gravels toward the base. The grain sizes and structural properties of the sediments indicate that they were deposited first within channels (Unit 5), later at the channel/floodplain interface (Unit 4), and finally on the floodplain of the paleo-Hrazdan River (Units 3 to 1). Micromorphological analysis shows

that the alluvial layers are primarily composed of pyroclastic silt and sand. Unit 2 is the humic A horizon and Unit 3 the Bt horizon of a floodplain soil, whereas Unit 1 represents renewed alluvial deposition. Two unconformities exist within the alluvial sequence. The first, of unknown age and duration, is located at the contact between Units 2 and 1 and represents the missing O horizon of the floodplain soil profile. The second, located between Unit 1 and Basalt 1, is associated with the truncation of the former before the passage of the latter and represents roughly 100,000 years, based on $^{40}\text{Ar}/^{39}\text{Ar}$ dating of sanidine grains from cryptotephra obtained from the uppermost 5 cm of Unit 1 (308 ± 3 ka) (Fig. 2, fig. S9, and databases S1 and S2). A third unconformity is documented at the contact between Unit 5 and Basalt 7.

Strong links between paleoclimate variations and environmental changes have been identified at Early Pleistocene localities within the region and show that the environmental responses to past climate changes in western Asia were broadly comparable to those from Europe and the Mediterranean, with cooler and drier glacial periods, and warmer and more humid interglacials (29, 30). Pedogenic processes in the Southern Caucasus probably coincided with warm, humid interglacials that led to soil development over most of Europe and vast parts of Asia. Consequently, based on the $^{40}\text{Ar}/^{39}\text{Ar}$ ages of the Unit 1 tephra and Basalt 7 and the unconformity identified between Units 1 and 2, we correlate the deposition of Units 5 to 4 with late OIS 10/early OIS 9e, deposition of and pedogenesis within Units 3 to 2 with OIS 9e (335 to 325 ka), and accretion of the overlying truncated basal remnant of Unit 1 with OIS 9c/b (Fig. 3).

The NG1 lithic assemblage (Fig. 4, table S5, and figs. S10 to S14) is produced entirely on obsidian, and all stages of reduction and manufacture are represented. All cores exhibit a volumetric core concept, with hierarchically organized surfaces separated by a plane of intersection. Seven-

teen of these cores conform to criteria that define Levallois technology (14, 15), and both the preferential and recurrent Levallois methods are present. Core dorsal scar patterns are predominantly unidirectional, bidirectional, and centripetal, and débordants document the management of core flake release surfaces. Levallois flakes and blades typically exhibit plain or faceted platforms, and dorsal scar patterns are principally unidirectional with evidence at their distal extremities for the lateral and distal preparation of the cores from which they were detached. The bifaces are of variable sizes and morphologies; however, the larger specimens are morphologically similar to Late Acheulian bifaces found throughout Eurasia. Scrapers of various types (e.g., déjeté

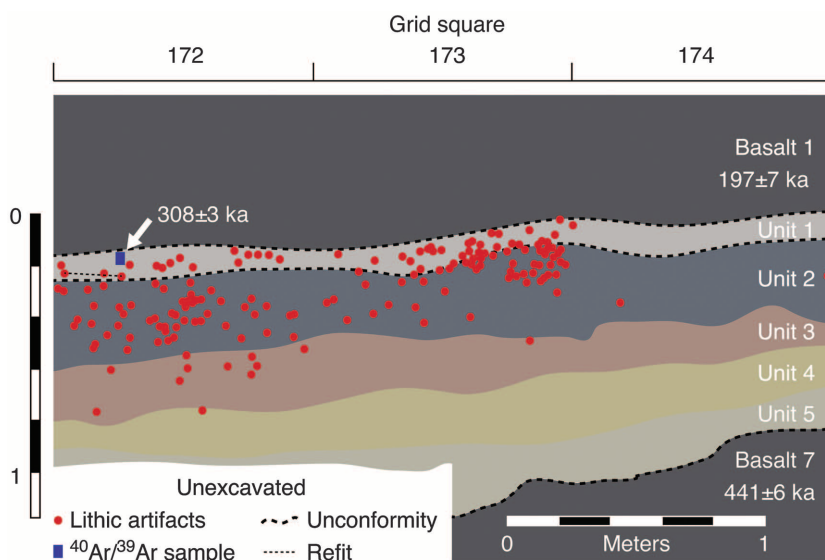


Fig. 2. Representative stratigraphic section of NG1. See figs. S4 and S5 for section location.

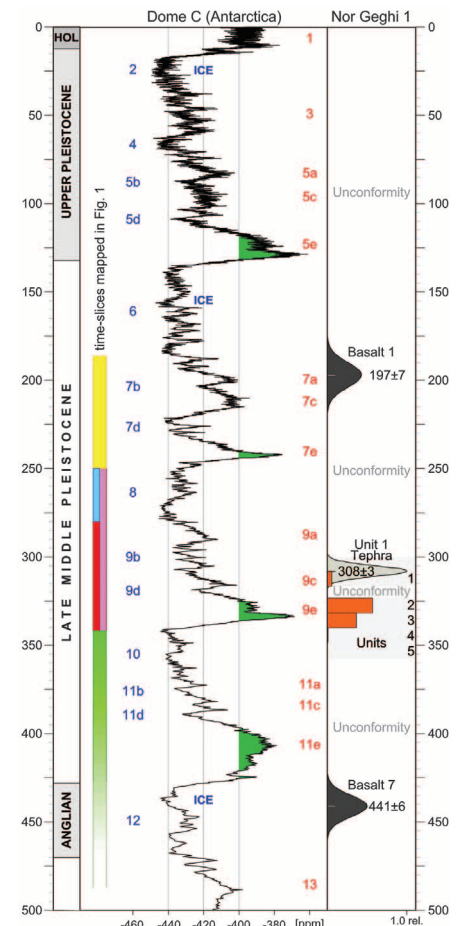


Fig. 3. Age model of the NG1 geostratigraphic sequence. The sequence is based on the $^{40}\text{Ar}/^{39}\text{Ar}$ age chronology, stratigraphic, and micromorphological results, correlated with the last 500 ka of the European Project for Ice Coring in Antarctica Dome C deuterium isotope record of Pleistocene climate change [δD [parts per million] (ppm) (38)]. Left/even blue numbers indicate cold dry stages; right/odd red numbers indicate warm, humid stages; and green shading (δD levels > -400 ppm) indicates peak interglacial periods, during which most of Europe was densely forested.

and transverse, with Quina retouch) dominate the retouched tool assemblage, and resharpening flakes indicate the onsite production and maintenance of these implements.

The elemental composition of 316 artifacts was measured nondestructively using portable x-ray fluorescence (pXRF) (31). The results indicate that 93.7% of the artifacts derive from the Gutasar volcano obsidian flows (2 to 8 km northeast), 2.8% from Hatis (12 km east-southeast), 3.2% from Pokr Arteni (70 km west), and 0.3% from Pokr Sevkar (120 km southeast) (figs. S15 and S16). The latter two sources are located within distant drainages not linked to the Hrazdan, and therefore hominin transport is the only mechanism to explain their presence at NG1. The procurement of obsidian from a variety of local and

nonlocal sources suggests that hominins at NG1 were exploiting large, environmentally diverse territories.

Early evidence for Levallois technology is found in assemblages from Western Europe dated to late OIS 9 and perhaps earlier (Fig. 1 and table S6), but these are often from secondary contexts or assigned to the “Final Acheulian” because of the presence of bifaces and the low frequency or absence of the preferential Levallois method. In addition, these assemblages lack the Quina scrapers that in part define the AY, where the Levallois method is rare or absent (32). The lithic assemblage from NG1 is unique in its combination of bifacial and Levallois technology, with Quina retouch and blade production, all recovered from a secure stratigraphic context.

Given the absence of taphonomic mixing, the intimate archaeological association of these technologies and artifact types could result from multiple hominin groups with distinct lithic traditions occupying NG1 alternately over thousands of years, thus producing a “mixed” lithic signature. However, this hypothesis would require us to accept that LMP hominins were less technologically flexible than indicated by the African and Eurasian archaeological evidence (6, 33, 34). Our data are consistent with the hypothesis that the synchronic technological variance documented at NG1 reflects the behavioral variability and technological evolution of a local Late Acheulian population and are thus inconsistent with the expectations and assumptions of the single-origin and dispersal model for Levallois technology.

Empirical evidence supports the contention that Levallois technology is an inherent property of the Acheulian that evolves out of the existing, but previously separate technological systems of *façonnage* and *débitage* (7, 35), and shows that Acheulian bifacial technology and Levallois technology are homologous, reflecting an ancestor-descendant relationship (36). Rather than a “technical breakthrough” that spread from a single point of origin, Levallois technology resulted from the gradual synthesis of stone knapping behaviors shared among hominins in Africa and those indigenous to the Acheulian dispersal area in Eurasia (Fig. 1). Consequently, the development of Levallois technology within Late Acheulian contexts represents instances of technological convergence.

The geographically and temporally discontinuous pattern of early Levallois technology and the presence of Acheulian-like assemblages in the LMP (\leq late OIS 6) suggest that hominins shifted between different technological options and/or that technological change was not always maintained, perhaps due to small effective population sizes, geographically restricted social networks, or high extinction rates (35). The eventual proliferation of Levallois technology during OIS 8 to OIS 7 and its continued ubiquity into late OIS 3 (Fig. 1 and table S6) establish it as an evolutionarily significant adaptation practiced by diverse hominin populations irrespective of taxonomic affiliation or environment. As such, variations in lithic technology cannot be considered proxies for hominin demographic changes during the LMP. At NG1, the early synchronic use of bifacial and Levallois technology is consistent with the hypothesis that developments in the technological realm of LMP hominins resulted from deep-rooted evolutionary processes based on a common technological ancestry.

REFERENCES AND NOTES

1. McDougall, F. H. Brown, J. G. Fleagle, *Nature* **433**, 733–736 (2005).
2. J. J. Hublin, *Proc. Natl. Acad. Sci. U.S.A.* **106**, 16022–16027 (2009).
3. G. Clark, *World Prehistory: A New Outline* (Cambridge Univ. Press, London, 1969).
4. N. Porat et al., *J. Archaeol. Sci.* **37**, 269–283 (2010).
5. A. I. R. Herries, *Int. J. Evol. Biol.* **2011**, 1–25 (2011).
6. C. A. Tryon, J. T. Faith, *Curr. Anthropol.* **54** (S8), S234–S254 (2013).

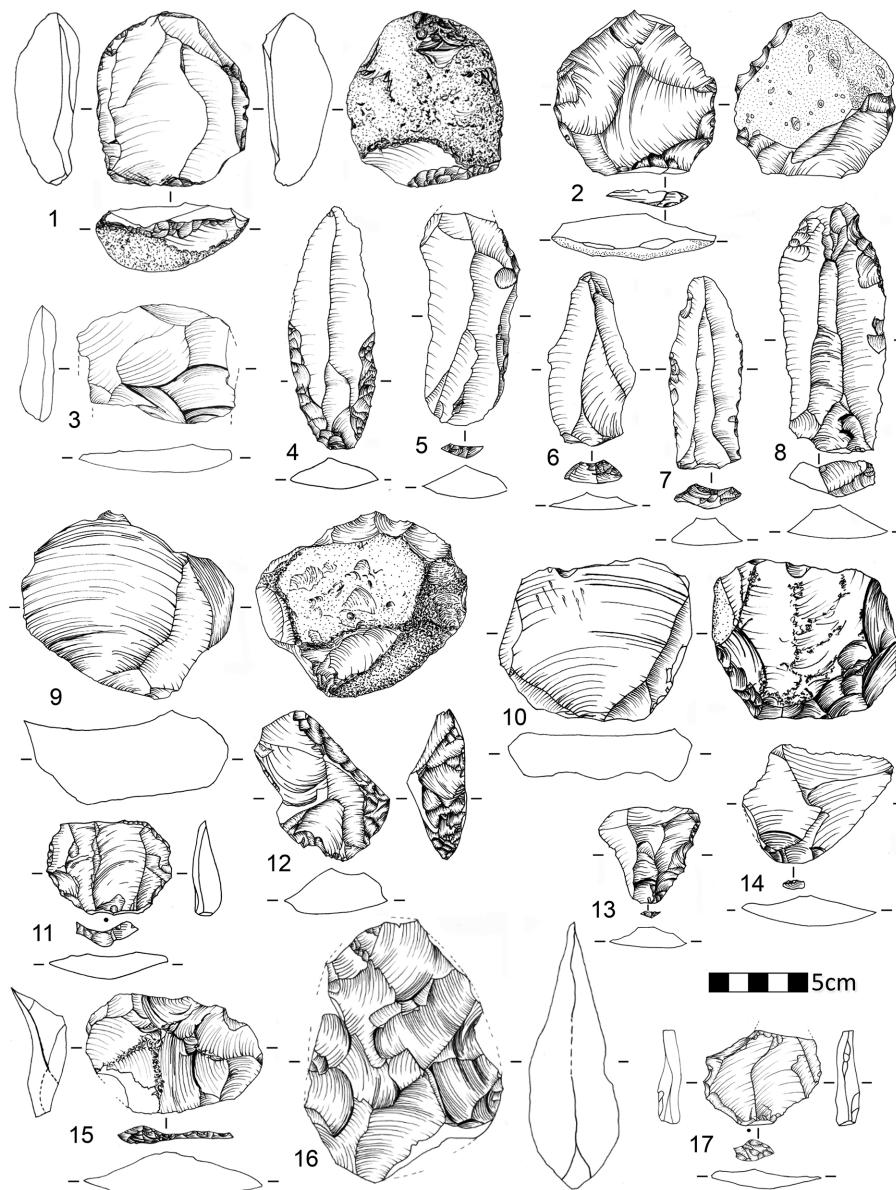


Fig. 4. Obsidian artifacts from NG1. Levallois: 1 and 2, recurrent cores; 3, 11, 13 to 15, and 17, flakes; 4, point with retouched base; 5 to 8, blades; 9 and 10, preferential cores. Non-Levallois: 12, scraper with Quina retouch; 16, biface.

7. M. White, N. Ashton, *Curr. Anthropol.* **44**, 598–609 (2003).
8. F. Fontana et al., *J. Anthropol. Archaeol.* **32**, 478–498 (2013).
9. A. Picin, M. Peresani, C. Falguères, G. Gruppioni, J.-J. Bahain, *PLOS ONE* **8**, e76182 (2013).
10. R. Barkai, A. Gopher, S. E. Lauritzen, A. Frumkin, *Nature* **423**, 977–979 (2003).
11. R. Shimelmitz, R. Barkai, A. Gopher, *J. Hum. Evol.* **61**, 458–479 (2011).
12. S. L. Kuhn, *Curr. Anthropol.* **54**, S255–S268 (2013).
13. V. B. Doronichev, *PaleoAnthropol.* **2008**, 107 (2008).
14. E. Boëda, in *The Definition and Interpretation of Levallois Technology*, H. L. Dibble, O. Bar-Yosef, Eds. (Prehistory Press, Madison, WI, 1995), pp. 41–69.
15. E. Boëda, *Le Concept Levallois: Variabilité des Méthodes* (CNRS Éditions, Paris, 1994).
16. P. J. Brantingham, S. L. Kuhn, *J. Archaeol. Sci.* **28**, 747–761 (2001).
17. S. J. Lycett, M. I. Eren, *J. Archaeol. Sci.* **40**, 2384–2392 (2013).
18. S. J. Lycett, M. I. Eren, *World Archaeol.* **45**, 519–538 (2013).
19. M. I. Eren, S. J. Lycett, *PLOS ONE* **7**, e29273 (2012).
20. R. Foley, M. M. Lehr, *Camb. Archaeol. J.* **7**, 3 (1997).
21. S. J. Armitage et al., *Science* **331**, 453–456 (2011).
22. H. Valladas et al., *J. Hum. Evol.* **65**, 585–593 (2013).
23. M. Meyer et al., *Nature* **505**, 403–406 (2014).
24. K. Prüfer et al., *Nature* **505**, 43–49 (2014).
25. Materials and methods are available as supporting material on Science Online.
26. R. Badalian et al., *Radiat. Meas.* **34**, 373–378 (2001).
27. E. V. Arutyunyan, V. A. Lebedev, I. V. Chernyshev, A. K. Sagatelyan, *Dokl. Earth Sci.* **416**, 1042–1046 (2007).
28. V. A. Lebedev, I. V. Chernyshev, K. N. Shatagin, S. N. Bubnov, A. I. Yakushev, *J. Volcanol. Seismol.* **7**, 204–229 (2013).
29. S. Joannin et al., *Earth Planet. Sci. Lett.* **291**, 149–158 (2010).
30. V. Ollivier et al., *Quat. Int.* **223–224**, 312–326 (2010).
31. E. Frahm et al., *J. Archaeol. Sci.* **41**, 333–348 (2014).
32. A. J. Jelinek, *Science* **216**, 1369–1375 (1982).
33. S. McBrearty, *J. Archaeol. Res.* **69**, 7 (2013).
34. J. J. Shea, *Curr. Anthropol.* **52**, 1–35 (2011).
35. T. Hopkinson, A. Nowell, M. White, *PaleoAnthropology* **2013**, 61 (2013).
36. S. Lycett, *J. Anthropol. Archaeol.* **26**, 541–575 (2007).
37. R. Stöckli, E. Vermote, N. Saleous, R. Simmon, D. Herring, The Blue Marble Next Generation - A true color earth dataset including seasonal dynamics from MODIS (NASA Earth Observatory, 2005); <http://earthobservatory.nasa.gov/Features/BlueMarble/bmng.pdf>.
38. L. Augustin et al., *Nature* **429**, 623–628 (2004).

ACKNOWLEDGMENTS

Data discussed in this paper can be found in the supplementary materials. All artifacts are stored at the Institute of Archeology and Ethnography, Yerevan, Armenia. We thank the following organizations for their financial support: the University of Connecticut [2008–2014: Norian Armenian Programs Committee, College of Liberal Arts and Sciences (CLAS), Office of Global Affairs, Study Abroad; and CLAS Book Committee]; the UK Natural Environment Research Council (grant IP-1186-0510), the L. S. B. Leakey Foundation (2010 and 2011), the Irish Research Council (2008 and 2009), and the University of Winchester. We also thank P. Avetisyan and B. Yeritsyan, Institute of Archeology and Ethnography, Republic of Armenia, for their collaboration.

SUPPLEMENTARY MATERIALS

www.sciencemag.org/content/345/6204/1609/suppl/DC1
Materials and Methods

Supplementary Text

Figs. S1 to S16

Tables S1 to S7

References (39–192)

Databases S1 and S2

27 May 2014; accepted 19 August 2014

10.1126/science.1256484

PALEONTOLOGY

Semiaquatic adaptations in a giant predatory dinosaur

Nizar Ibrahim,^{1*} Paul C. Sereno,¹ Cristiano Dal Sasso,² Simone Maganuco,² Matteo Fabbri,³ David M. Martill,⁴ Samir Zouhri,⁵ Nathan Myhrvold,⁶ Dawid A. Iurino⁷

We describe adaptations for a semiaquatic lifestyle in the dinosaur *Spinosaurus aegyptiacus*. These adaptations include retraction of the fleshy nostrils to a position near the mid-region of the skull and an elongate neck and trunk that shift the center of body mass anterior to the knee joint. Unlike terrestrial theropods, the pelvic girdle is downsized, the hindlimbs are short, and all of the limb bones are solid without an open medullary cavity, for buoyancy control in water. The short, robust femur with hypertrophied flexor attachment and the low, flat-bottomed pedal claws are consistent with aquatic foot-propelled locomotion. Surface striations and bone microstructure suggest that the dorsal “sail” may have been enveloped in skin that functioned primarily for display on land and in water.

Bones of the predatory dinosaur *Spinosaurus aegyptiacus* first came to light over a century ago from Upper Cretaceous rocks in Egypt (1–3) but were destroyed in World War II (4). More recently, isolated teeth and bones (5) and the anterior half of an adult skull (6) have been discovered in the Kem Kem beds of eastern Morocco (Fig. 1A) and equivalent horizons in Algeria, but are insufficiently complete to estimate the size, proportions, and

functional adaptations of this species. Here we report the discovery of a partial skeleton of *S. aegyptiacus* from the middle of the Kem Kem sequence (Fig. 1B), which is probably Cenomanian in age (~97 million years ago) (7).

The subadult skeleton, here designated the neotype of *S. aegyptiacus* (8), preserves portions of the skull, axial column, pelvic girdle, and limbs. It was discovered in fluvial sandstone that has yielded remains of the sauropod *Rebbachisaurus* (9) and three other medium-to-large theropods (an abelisaurid, *Deltadromeus*, and *Carcharodontosaurus*) (7, 10). We regard two additional Kem Kem theropods, *Sigilmassasaurus brevicollis* and *S. maroccanus* (11, 12), to be referable to *S. aegyptiacus* (8).

The neotype skeleton and isolated bones referable to *S. aegyptiacus* were scanned with computed tomography, size-adjusted, and combined with a digital recreation of the original Egyptian fossils (Fig. 2A, red). Missing bones were extrapolated between known bones or estimated from those of other spinosaurids (6, 13, 14). The digi-

tal model of the adult skeleton of *Spinosaurus* (Fig. 2A), when printed and mounted, measures over 15 m in length, longer than *Tyrannosaurus* specimens (~12.5 m) (15).

A concentrated array of neurovascular foramina open on the anterior end of the snout and appear similar to foramina in crocodylians that house pressure receptors that detect water movement (8, 16) (Fig. 2B and fig. S6). The enlarged, procumbent, interlocking anterior teeth are well adapted for snaring fish (5, 6) (Fig. 2B and fig. S4). The fossa for the fleshy nostril is small and, unlike any other nonavian dinosaur, is retracted to a posterior position to inhibit the intake of water (Fig. 2C and figs. S4 and S6) (8).

Most cervical and dorsal centra are elongate compared to the sacral centra, resulting in a proportionately long neck and trunk (Figs. 2A and 3 and tables S1 and S2). The anteriormost dorsal centra, however, are proportionately short, exceptionally broad, and concavoconvex (Fig. 2D). These characteristic vertebrae, the affinity of which has been controversial (7, 11, 12), are referred here to *S. aegyptiacus*, based on their association with spinosaurid skeletons in Niger (8) and Egypt (2). The horizontal cervicodorsal hinge created by these broad centra would facilitate dorsoventral excursion of the neck and skull in the pursuit of prey underwater.

The distal two-thirds of the tail comprises vertebrae with relatively short centra, diminutive zygapophyses, and anteroposteriorly compressed neural spines (Fig. 2G). The affinity of these caudal elements has been uncertain (17), but comparisons with associated remains from Egypt (2) and more proximal caudals in the neotype (Fig. 2A) allow referral to *Spinosaurus*. Short centra and reduced neural arch articulations enhance lateral bending during tail propulsion in bony fish (18).

The forelimb has hypertrophied deltopectoral and olecranon processes for powerful flexion and extension (Fig. 2A). Elongate manual phalanges (Fig. 2H) and less recurved, manual unguals that

¹Department of Organismal Biology and Anatomy, University of Chicago, Chicago, IL 60637, USA. ²Museo di Storia Naturale di Milano, Corso Venezia 55, 20121 Milan, Italy.

³School of Earth Sciences, University of Bristol, Queen's Road, Bristol, BS8 1RJ, UK. ⁴School of Earth and

Environmental Sciences, University of Portsmouth, Burnaby Road, Portsmouth, PO1 3QL, UK. ⁵Laboratoire de

Géosciences, Faculté des Sciences Ain Chock, Université Hassan II, Casablanca, Morocco. ⁶Intellectual Ventures, 3150 139th Avenue Southeast, Bellevue, WA 98005, USA.

⁷Dipartimento di Scienze della Terra, Sapienza Università di Roma, Piazzale Aldo Moro 5, 00185 Rome, Italy.

*Corresponding author. E-mail: nibrahim@uchicago.edu